Neuropsychopharmacology (2014) 39, 1664–1673

www.neuropsychopharmacology.org

Long-Term Memory Deficits are Associated with Elevated Synaptic ERK1/2 Activation and Reversed by mGluR5 Antagonism in an Animal Model of Autism

Ronald R Seese[1], Anna R Maske[1], Gary Lynch[1,2] and Christine M Gall*[,1,3]

[1]Department of Anatomy and Neurobiology, University of California, Irvine, CA, USA; [2]Department of Psychiatry and Human Behavior, University of California, Irvine, CA, USA; [3]Department of Neurobiology and Behavior, University of California, Irvine, CA, USA

A significant proportion of patients with autism exhibit some degree of intellectual disability. The BTBR T^+ *Itpr3*^{tf}/J mouse strain exhibits behaviors that align with the major diagnostic criteria of autism. To further evaluate the BTBR strain's cognitive impairments, we quantified hippocampus-dependent object location memory (OLM) and found that one-third of the BTBR mice exhibited robust memory, whereas the remainder did not. Fluorescence deconvolution tomography was used to test whether synaptic levels of activated extracellular signal-regulated kinase 1/2 (ERK1/2), a protein that contributes importantly to plasticity, correlate with OLM scores in individual mice. In hippocampal field CA1, the BTBRs had fewer post-synaptic densities associated with high levels of phosphorylated (p-) ERK1/2 as compared with C57BL/6 mice. Although counts of p-ERK1/2 immunoreactive synapses did not correlate with OLM performance, the intensity of synaptic p-ERK1/2 immunolabeling was negatively correlated with OLM scores across BTBRs. Metabotropic glutamate receptor (mGluR) 5 signaling activates ERK1/2. Therefore, we tested whether treatment with the mGluR5 antagonist MPEP normalizes synaptic and learning measures in BTBR mice: MPEP facilitated OLM and decreased synaptic p-ERK1/2 immunolabeling intensity without affecting numbers of p-ERK1/2+ synapses. In contrast, semi-chronic ampakine treatment, which facilitates memory in other models of cognitive impairment, had no effect on OLM in BTBRs. These results suggest that intellectual disabilities associated with different neurodevelopmental disorders on the autism spectrum require distinct therapeutic strategies based on underlying synaptic pathology.
Neuropsychopharmacology (2014) **39,** 1664–1673; doi:10.1038/npp.2014.13; published online 12 February 2014

Keywords: BTBR; *Fmr1* KO; object location memory; cAMP response element binding protein (CREB); positive AMPA receptor modulator (ampakine); MPEP

INTRODUCTION

Autism is a prevalent neurodevelopmental disorder, affecting approximately 1 in 100 people. A significant proportion of persons diagnosed with autism exhibit intellectual disability, yet no effective treatment exists for these cognitive impairments (Baio, 2012; Bryson *et al*, 2008; Fombonne, 2006; La Malfa *et al*, 2004). The complex phenotypes of autism are difficult to model in mice (Moy *et al*, 2006; Patterson, 2011; Silverman *et al*, 2010b), thereby slowing the development of successful therapies. Nonetheless, the three diagnostic criteria of autism (eg, impaired sociability, abnormal communication, and excessive stereotypic behaviors) are expressed by the BTBR T^+ *Itpr3*^{tf}/J (formerly BTBR T^+ *tf*/J and hereafter 'BTBR') inbred strain (McFarlane *et al*, 2008; Meyza *et al*, 2013; Scattoni *et al*, 2011). These findings indicate that the BTBR strain might be a useful model for aspects of idiopathic (polygenetic) autism.

To understand the neurobiological basis of intellectual disability, including that associated with autism, it is critical to study synapses, as these sites exhibit plasticity thought to underlie learning. There is now a large literature demonstrating disturbances in spine morphology and signaling cascades at excitatory synapses in animal models of cognitive disability (Belichenko *et al*, 2007; Kramar *et al*, 2012), including disorders on the autism spectrum (Chen *et al*, 2010; Hung *et al*, 2008; Seese *et al*, 2012; Tropea *et al*, 2009). Learning and executive functions are impaired in BTBR mice (Amodeo *et al*, 2012; Lipina and Roder, 2013; MacPherson *et al*, 2008; Ribeiro *et al*, 2013; Rutz and Rothblat, 2012; Silverman *et al*, 2013; Yang *et al*, 2012), but thorough analyses of associated synaptic abnormalities and evidence for pharmacological normalization of these measures are lacking.

The present studies addressed these issues. We used the hippocampus-dependent object location memory (OLM) task to compare memory in BTBRs and C57BL/6 mice, and

*Correspondence: Dr CM Gall, Department of Anatomy and Neurobiology, School of Medicine, University of California, Irvine, CA 92697-1275, USA, Tel: +1 949 824 8652, Fax: +1 949 824 1255, E-mail: cmgall@uci.edu
Received 17 November 2013; revised 31 December 2013; accepted 7 January 2014; accepted article preview online 22 January 2014

fluorescence deconvolution tomography to determine whether strain effects on cognitive performance are associated with abnormalities in synaptic signaling of extracellular signal-regulated kinase (ERK) 1/2, a protein critical for long-term memory (Thomas and Huganir, 2004) and disturbed in forms of autism and its models (Hou *et al*, 2006; Michalon *et al*, 2012; Samuels *et al*, 2009; Seese *et al*, 2012; Zou *et al*, 2011). The results show that poor learning performance is associated with disturbances in ERK1/2 signaling in BTBRs and that both measures are amenable to normalization with pharmacological treatments.

MATERIALS AND METHODS

Animals and Behavioral Analyses

Studies used adult (4–6 month old) male BTBR (McFarlane *et al*, 2008) and age- and sex-matched C57BL/6 mice (hereafter 'B6') from colonies established with breeders from Jackson Laboratory. B6 mice were chosen for comparison with BTBRs because they are extensively used in behavioral genetics, exhibit high levels of social approach (Bolivar *et al*, 2007; McFarlane *et al*, 2008; Yang *et al*, 2007), and have been used for comparison with BTBRs in previous work (Babineau *et al*, 2013; Silverman *et al*, 2013; Wohr *et al*, 2011; Yang *et al*, 2012). Mice were standard group-housed with littermates in rooms maintained at 68 °C and 55% humidity, with 12 h on/12 h off light cycle, and food and water *ad libitum*. Each experiment used behaviorally naive mice and ran all groups through behavioral analyses together. Experiments were performed on the animal's light cycle between 0800 hours and noon, in an otherwise dark room with dimmed overhead lighting (235 lux), and in accordance with NIH guidelines for the care of laboratory animals and institutionally approved protocols.

Mice were palm handled for 2 min daily for 5 days and then habituated to a white arena (30 × 24 cm floor; 30 cm walls) containing sawdust for 5 min daily for 5 days (Haettig *et al*, 2011). Animals were palm, as opposed to tail, handled to minimize anxiety from transfer to and from the testing arena (Hurst and West, 2010). Mice were then subject to a 5 min arena-training episode in which identical 100 ml glass beakers were placed in two corners, approximately 1 inch from the perimeter. For the 5 min long retention test conducted 24 h after training, one beaker remained in its training location and the second beaker was placed in the center of the apparatus. The arena was cleaned after each use feces were removed, sawdust was mixed, and beakers were cleaned with 70% ethanol.

During all episodes of arena use, the mice were video recorded with an overhead camera 4 feet above the chamber, and movements tracked live using ANY-Maze software (Stoelting). Total exploration time (t) was quantified, by offline raters blind to treatment group, as the total time interacting with both objects. A discrimination index was also calculated as $(t_{\text{novel}} - t_{\text{familiar}})/(t_{\text{novel}} + t_{\text{familiar}}) \times 100$. A positive discrimination index reflects a preference for the moved object's novel location.

Mice were scored as interacting with an object when sniffing and with nose touching the object or within 0.5 inches from the object. Interaction was not scored (a) when the animal was within this radius but either grooming or digging, or (b) when the animal touched the object or was within this radius but did not show intent to interact (eg, they fell within this zone when turning). The timing of digging behavior was also quantified during training and retention trials; this included measures of latency to the first episode after entering the arena and the duration and frequency of episodes for each mouse. Average time per digging episode was calculated by dividing total summed digging time by digging frequency.

Drug Administration

All compounds were administered by intraperitoneal injection in a room adjacent to that used for behavioral testing. The positive AMPA receptor modulator CX929 (gift of Cortex Pharmaceuticals) was dissolved at 7.5 mg/ml in sterile 30% cyclodextrin (CDX) before being diluted with sterile 0.9% NaCl to a working concentration of 2.5 mg/ml in 10% CDX. Mice were injected twice daily (0900 hours and 1600 hours) with sterile saline (2 days), 10% CDX (4 days), and then either 10% CDX or CDX + CX929 (5 mg/kg; 4 days). The first injection was on the first day of handling and the final injection occurred on the afternoon of the fifth habituation day, approximately 17 h before training. This protocol was chosen because previous work has shown that it increases endogenous hippocampal brain-derived neurotrophic factor (BDNF) expression and promotes memory in both Huntington's disease and Angelman syndrome model mice (Baudry *et al*, 2012).

The metabotropic glutamate receptor 5 (mGluR5) antagonist 2-Methyl-6-(phenylethynyl)pyridine (MPEP) (gift of FRAXA) was dissolved in sterile saline to a final concentration of 2.5 mg/ml. Mice were injected once daily with saline (4 days) and then with saline or MPEP (5 mg/kg; 1 day). The first injection corresponded with the second day of habituation and the final injection, containing MPEP, was administered 30 min before training. This protocol and dose was selected because it reverses other behavioral abnormalities of BTBR mice (Silverman *et al*, 2010a).

Immunohistochemistry and Image Analysis

For studies of ERK1/2 signaling, mice were euthanized with isoflurane and decapitated. Brains were fast frozen in −50 °C 2-methylbutane and cryostat sectioned (20 μm, coronal) to generate multiple series of evenly spaced sections through hippocampus. The slide-mounted tissue was processed for dual immunofluorescence (Seese *et al*, 2012) including overnight incubation in primary antisera cocktail containing mouse anti-PSD95 (1:1000, Pierce) and rabbit antisera to p-ERK1/2 Thr202/Tyr204 (1:500, Cell Signaling), ERK1/2 (1:500, Cell Signaling), or p-CREB Ser133 (1:250, Millipore). Secondary antisera included donkey anti-mouse AlexaFluor488 and donkey anti-rabbit AlexaFluor594. Sections were cover slipped using Vecta-Shield with DAPI (Vector labs).

Digital image Z-stacks were collected through 3 μm (0.2 μm steps) using a Leica DM6000 epifluorescence microscope and ×63 oil-immersion objective (NA 1.4). The 136 × 105 μm sample fields were centered in hippocampal field CA1b stratum radiatum. Two to three Z-stacks were acquired from each tissue section, and four to five

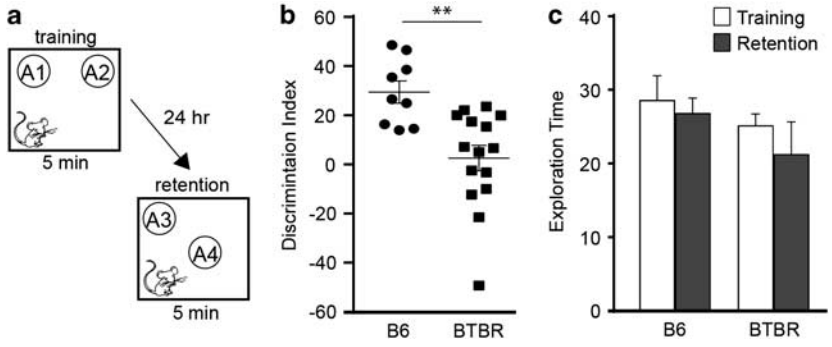

Figure 1 Long-term object location memory (OLM) is impaired in BTBR mice. (a) Following handling and habituation, adult male C57BL/6 (B6) and BTBR mice were subjected to 5 min 'training' during which two identical objects (A1 and A2) were placed in the corners of the apparatus. One day later, mice were tested for OLM 'retention' : the same objects were used with one in the 'familiar' location experienced during training (A3) and one placed in a 'novel' location (A4). (b) Discrimination indices of the OLM retention trial show a robust difference between strains (values for individual mice plotted, line denotes the group mean ± SEM; Mann-Whitney test, $P<0.002$; $N\geqslant 9$/group). Despite the strain difference, a small subgroup of BTBR mice performed at the level of B6s. (c) Bar graph shows that mean exploration times (in seconds) were not different between strains on either the training ($P=0.32$) or retention ($P=0.36$) trial.

sections, at planes 1.6 mm to -2.5 mm from Bregma, were imaged for each mouse. Z-stacks were processed for restorative deconvolution and construction of 3D montages of each 42 840 μm^3 sample field (Volocity 5.0, Perkin Elmer). Automated systems then counted and measured the fluorescence intensities of single- and double-labeled elements that met size and eccentricity constraints of synapses (Seese *et al*, 2012; Seese *et al*, 2013). Contacts were counted as double labeled if there was any overlap in their immunolabeled boundaries as evaluated in 3D. Counts of densely ERK1/2 immunopositive (+) PSDs were normalized to the total number of PSD95+ elements in a given sample field; these normalized values from each Z-stack were averaged to obtain a mean value for each brain. For each animal, frequency distributions of the intensities of all immunolabeled elements were derived; median intensity values were used as a measure of central tendency because this measure is least strongly influenced by skewed or non-normal distributions.

Sample Preparation and Western Blotting

Adult (4 mo old) male B6 and BTBR mice were deeply anesthetized with isoflurane and decapitated. Only male mice were used to prevent effects of the estrus cycle on memory-encoding processes. The two hippocampi were pooled, homogenized in ACSF containing 1× Protease Inhibitor Cocktail (Roche) and 1× Phosphatase Inhibitors 1 and 2 (Sigma) and run for western blot analysis.

Synaptoneurosomes were isolated from male and female C57BL/6 WT and BTBR mice at 14–16 days of age (Bernard-Trifilo *et al*, 2005; Seese *et al*, 2012). Both sexes from these pre-pubertal animals were used to increase yield. Approximately 15 µg of protein was run for 10% PAGE western blot analysis.

Blots were incubated overnight at 4 °C in primary antisera including mouse antisera to actin (1:10 000, Sigma) and p-ERK1/2 Thr202/Tyr204 (1:1500; Cell Signaling) and rabbit antisera to ERK1/2 (1:2500, Cell Signaling) and p-CREB Ser133 (1:2500, Millipore). Bands were visualized using ECL+ chemiluminescence (Amersham), quantified using ImageJ (NIH), and normalized to sample actin content.

Statistical analysis

All groups were tested for normality using the D'Agostino & Pearson omnibus normality test or the Kolmogorov-Smirnov test. For groups that failed these tests (alpha = 0.05), non-parametric statistical comparisons (Mann–Whitney test (MW), Spearman correlations) were performed. Otherwise, parametric tests (Student's *t*-test, Pearson correlations) were used. Sigmoidal fits to cumulative probability distributions of immunolabeling intensities were generated in Prism 6 (GraphPad); the slopes at the distributions' inflection points ('Hill slopes') were then compared between groups. Holm-Sidak *post hoc* tests were performed for all ANOVAs. Statistical significance was considered as $P\leqslant 0.05$. A single *N* was an animal for behavioral and immunohistochemical analyses, and an independently treated sample for synapto-neurosomes. Unless otherwise specified, the Student's *t*-test was used for statistical comparisons, and values in text and figures are group means ± S.E.M.

RESULTS

Hippocampus-dependent Memory is Impaired in a Subgroup of BTBR mice

Adult B6 WT and BTBR mice were first tested for long-term OLM (Figure 1a). Mice were given one 5-min training episode and tested for retention 24 h later. B6 mice exhibited robust preference for the novel location object, as evidenced by a strongly positive discrimination index (DI). In contrast, as a group, the BTBR mice performed significantly worse than the B6s on the retention trial (MW, $P<0.002$; Figure 1b). This was not due to disinterest in exploration; BTBR mice interacted with the objects to a comparable degree as the B6s (training: $P=0.32$, retention: $P=0.36$; Figure 1c).

A noticeable behavior of the BTBR mice was excessive digging through the bedding in the behavioral apparatus, but not in the home cage. Although B6 mice also exhibit this behavior, the BTBRs spent a threefold greater time digging (training: $P=0.03$, retention: $P=0.02$; Figure 2a). A similar strain difference was seen for digging bout frequency

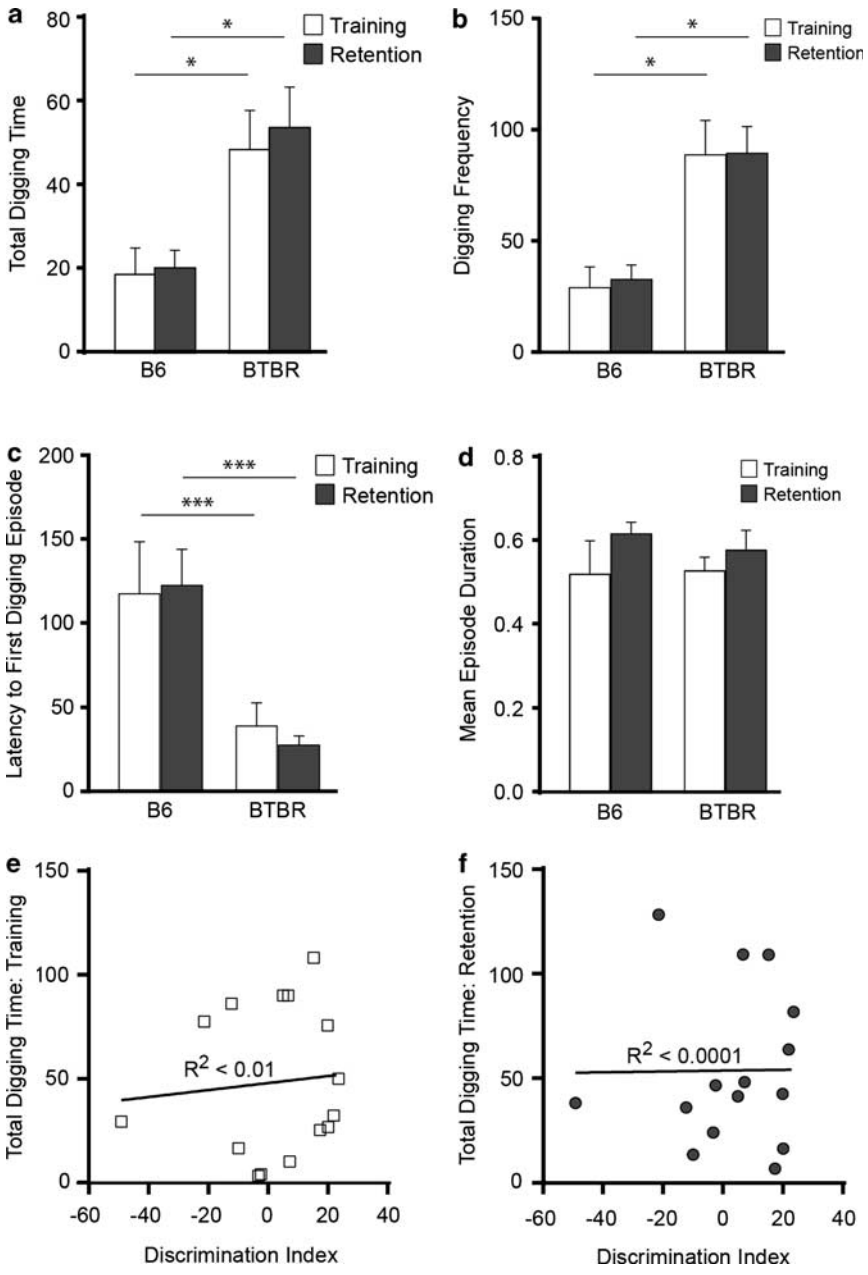

Figure 2 A repetitive stereotypic behavior is not associated with OLM impairments in BTBR mice. (a) Bar graphs shows that, as compared to B6 mice, BTBRs spend three times as much time digging (in seconds) through bedding on both training and retention trials (*$P<0.05$). (b) In both 5-min training and retention trials, frequency of digging bouts was greater in BTBR mice, as compared with the B6s (*$P<0.05$). (c) Latency to the first digging episode, measured in seconds, was shorter in BTBR mice as compared with B6s in both training and retention trials (Mann-Whitney test, ***$P<0.001$). (d) The mean duration (in seconds) of each digging episode did not differ between strains. (e, f) Scatter plots show the relationship of stereotypic digging behavior with OLM in individual BTBR mice. Regression analyses show that OLM retention trial discrimination indices do not correlate with the total time digging during either the training (e; Spearman correlation, $P=0.82$) or the retention (f; Spearman correlation, $P=0.67$) trial. In all cases $N\geqslant 9$/group.

(training: $P=0.01$, retention: $P=0.02$; Figure 2b) and latency to the first digging episode (MW, training: $P=0.0004$; *t*-test, retention: $P=0.00003$; Figure 2c), although the average time per episode was comparable between strains (MW, $P>0.90$ for training and retention trials; Figure 2d). We tested the prediction that these repetitive behaviors interfere with memory encoding in BTBRs by first assessing the correlation between an animal's retention trial DI and its time spent digging during training or retention testing (Figure 2e and f). Regression analyses did not detect significant correlations (Spearman correlations, training: $R^2=0.004$, $P=0.82$; retention: $R^2=0.13$, $P=0.65$). Further, removal of bedding from the apparatus did not enhance OLM in BTBRs: retention trial DIs with bedding absent (10.0 ± 5.5) were no different than when bedding was present (2.6 ± 5.1; MW, $P=0.49$). Thus, repetitive digging did not account for the deficiency in long-term OLM in BTBR mice.

Density of phospho-ERK1/2 is Abnormally Low in BTBR Synapses

Impaired hippocampal memory in BTBR mice suggests that synaptic signaling critical for encoding might be disturbed. We focused on ERK1/2 because (i) mutations in this kinase are associated with autism (Samuels *et al*, 2009), (ii) ERK1/2 levels are reportedly abnormal in BTBRs and other strains with autism-like phenotypes (Hou *et al*, 2006; Seese *et al*, 2012; Zou *et al*, 2011) and (iii) ERK1/2 activity is necessary for and activated by learning and memory (Thomas and Huganir, 2004). To test if ERK1/2 levels were abnormal at BTBR synapses, we employed fluorescence deconvolution tomography to quantify postsynaptic immunolabeling in CA1b fields containing ~40 000 postsynaptic densities (PSDs) (Seese *et al*, 2013). Sections from B6 and BTBR mice were immunolabeled for ERK1/2 and PSD95, a protein concentrated exclusively at excitatory synapses in field CA1 (Aoki *et al*, 2001); contacts were quantified for fields in CA1b stratum radiatum. Counts of all synapse-sized ERK1/2+ elements, and those double-labeled for PSD95, were not different between strains ($P=0.29$; Figure 3a). To corroborate these *in situ* findings biochemically, we evaluated ERK1/2 levels in hippocampal homogenates and forebrain synaptoneurosomes from B6 and BTBR mice. In both preparations, levels of ERK1/2 immunoreactivity (ir) did not differ between strains (homogenates: $P=0.61$, synaptoneurosomes: $P=0.55$; Figure 3b).

While overall ERK1/2 levels were not different between strains, it remained possible that synaptic ERK1/2 activation differed. Brain tissue sections were processed for dual immunofluorescence localization of phosphorylated (p-) ERK1/2 (Thr202/Tyr204) and PSD95, and labeled synapses were quantified as above. The effects of genotype were striking: total numbers of densely p-ERK1/2+ elements were similar (B6 *vs* BTBR: 38,049 ± 1,262 *vs* 38,627 ± 1262; $P=0.74$) but there were 60% fewer p-ERK1/2+ elements double labeled for PSD95 in the CA1 sample field of BTBRs as compared with B6 mice ($P=0.007$; Figure 3c). Synaptoneurosomal levels of p-ERK1/2 were also significantly lower in BTBRs ($P=0.03$; Figure 3d), whereas overall p-ERK1/2 levels were comparable ($P=0.25$).

To confirm that the above results reflect fewer synapses containing activated ERK1/2, we tested whether numbers of synapses containing phosphorylation of a canonical downstream substrate of ERK1/2, cAMP response element-binding protein (CREB), were also lower in BTBRs. Tissue sections were immunolabeled for PSD95 and the p-CREB Ser133 site targeted by ERK1/2 (Yu and Yezierski, 2005). Although the total numbers of p-CREB+ elements were not different between strains (B6, 36115 ± 1255; BTBR, 33341 ± 1548; $P=0.29$), in field CA1 densely p-CREB+ PSDs were 60% less abundant in BTBRs ($P=0.002$; Figure 3e). As with measures of p-ERK1/2, synaptoneurosomal, but not total, p-CREB-ir was lower in BTBR as compared with B6 mice (hippocampal homogenates: $P=0.94$; forebrain synaptoneurosomes: $P=0.00002$; Figure 3f).

Together, these findings indicate that in CA1 stratum radiatum the incidence of PSDs associated with activated ERK1/2 is lower in BTBR as compared with B6 mice.

Synaptic p-ERK1/2 Content is Correlated with Long-Term Memory in BTBR Mice

Although discrimination indices for OLM were lower for BTBR than B6 mice when group means were compared, the performance of BTBRs varied with clear high- and low-performing subpopulations. This broad performance distribution raised the question of whether synaptic p-ERK1/2 levels correlate with the integrity of hippocampus-dependent cognitive function in this strain. To address this possibility, well-handled BTBR mice were given 5-min training in the OLM task and tested for retention 24 h later. One week later the brains of these mice were collected and processed for fluorescence deconvolution tomography to evaluate p-ERK1/2 and PSD95 immunolabeling in CA1 stratum radiatum. Comparing OLM retention scores and the *number* of densely p-ERK1/2+ PSDs in BTBR mice (Figure 4a), however, yielded a nonsignificant Pearson correlation coefficient (Pearson correlation, $R^2=0.002$, $P=0.89$).

Although the number of densely p-ERK1/2+ synapses might influence processes not directly quantified by the DI, the *amount* of activated ERK1/2 at individual synapses might more strongly correlate with OLM performance. To test this possibility we quantified, for the same mice, p-ERK1/2 immunolabeling intensities for elements double labeled with PSD95. There was a significant negative correlation between BTBR retention trial DIs and median intensities of p-ERK1/2 immunolabeling of PSD95+ elements (Range of intensities: 86.6–91.4; mean ± SD of median intensities: 88.6 ± 1.4; Pearson correlation of intensities to retention trial discrimination indices: $R^2=0.26$, $P=0.05$; Figure 4b). These data support the notion that the poorer-performing BTBRs have higher postsynaptic p-ERK1/2 levels than do better-performing BTBR mice. We confirmed this prediction by dividing the BTBR mice into high- and low-performing groups based on being 1 SD from the mean DI of B6s (mean ± SD: 22.7 ± 8.7) simultaneously tested. Applying these criteria illustrated that 5 of the 15 BTBR mice qualified as high performing (DIs: 33.5 ± 5.79), whereas 10 were in the low-performing group (DIs: −0.2 ± 13.38). We then compared synaptic p-ERK1/2+ immunolabeling intensities between these groups. The low-performing mice exhibited a rightward shift toward higher p-ERK1/2 immunolabeling densities (Figure 4c) and greater median synaptic p-ERK1/2 immunolabeling intensities (mean ± SD of median intensities: 87.3 ± 0.4 (high-performing), 89.2 ± 0.4 (low-performing); $P=0.006$) as compared with high-performing mice. Cumulative fluorescence intensity frequency distributions were derived from these plots (Supplementary Figure S1) and sigmoidal fits (Goodness of Fit $R^2>0.999$ for both curves) demonstrated that slopes at the midpoints of curves ('Hill slopes') for the high- and low-performing groups were markedly different ($P<0.0001$). These results support the idea that *synaptic* ERK1/2 phosphorylation predicts long-term OLM performance in the BTBR mice, with higher densities of p-ERK1/2 associated with poorer performance.

mGluR5 Antagonism Rescues Memory and Normalizes p-ERK1/2 Content at BTBR Synapses

We next tested if therapeutics that restore learning in other models of cognitive impairment are effective in the BTBRs.

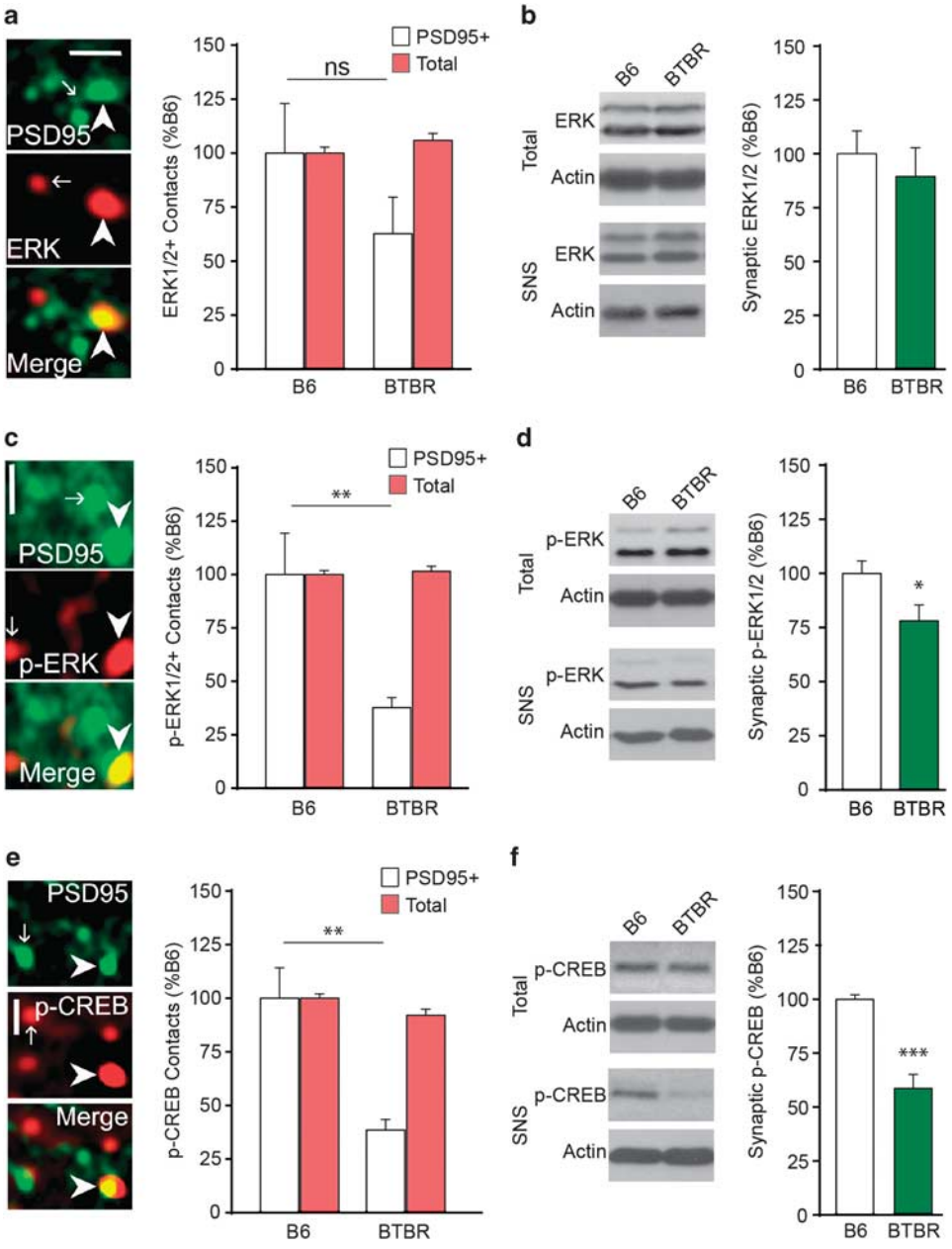

Figure 3 The number of stratum radiatum PSDs containing activated ERK1/2 is lower in BTBR as compared to B6 mice. (a) Left, Photomicrograph shows immunolabeling for total ERK1/2, PDS95 (a marker of excitatory synapses), and a merge of the two (bar = 1 μm for a,c,e). Arrows and arrowheads indicate single- and double-labeled elements, respectively. Right, both the number of ERK1/2 immunopositive (+) elements associated with PSD95 immunoreactivity (ir) (white bars) as well as the total number of ERK1/2 + elements (red bars) did not differ between B6 and BTBR mice ($N \geqslant 5$/group; here and in *B-F*, BTBR values are presented as percent of mean values from B6 mice). (b), Left, representative western blots of hippocampal homogenates and forebrain synaptoneurosomal fractions (SNS) show comparable levels of ERK1/2-ir in samples from B6 and BTBR mice. Right, quantification of blot band densities, normalized to sample actin content, confirmed no effect of strain on total ERK1/2-ir in SNS ($N \geqslant 5$/group). (c) Left, photomicrograph shows immunolabeling for phosphorylated (p-) ERK1/2 Thr202/Tyr204, PSD95, and a merge of the two. Right, quantification shows that in the CA1 stratum radiatum sample field, BTBR mice exhibit fewer PSD95 + contacts containing dense p-ERK1/2-ir than do B6 mice (**$P < 0.01$), whereas total numbers of p-ERK1/2 immunoreactive elements were not different between strains ($N \geqslant 9$/group). (d) Left, blots of hippocampal homogenates and forebrain SNS show levels of p-ERK1/2-ir and actin-ir in samples from B6 and BTBR mice. Right, densitometry of p-ERK1/2 immunoreactive bands (normalized to sample actin content) confirmed that SNS levels are lower in BTBR mice, as compared with B6s (*$P < 0.05$; $N \geqslant 9$/group). (e), Left, photomicrograph of immunolabeling for p-CREB Ser133, PSD95, and merged. Right, quantification of synapse-sized elements confirm that number of p-CREB + PSDs in CA1 stratum radiatum is lower in BTBR as compared with B6 mice (**$P < 0.01$), and that this difference was not seen for overall numbers of p-CREB + puncta ($N \geqslant 9$/group). (f) Left, blots of hippocampal homogenates and forebrain SNS show lower levels of p-CREB at synapses in BTBRs as compared with B6 mice; this was confirmed by blot densitometry (Right; $N \geqslant 9$/group).

Positive modulators of AMPA receptors ('ampakines') increase expression of BDNF (Simmons *et al*, 2009), a neurotrophin that regulates ERK1/2 signaling (Yoshii and Constantine-Paton, 2010). Semi-chronic treatment with the ampakine CX929 restores learning and hippocampal long-term potentiation in rodent models of Angelman syndrome

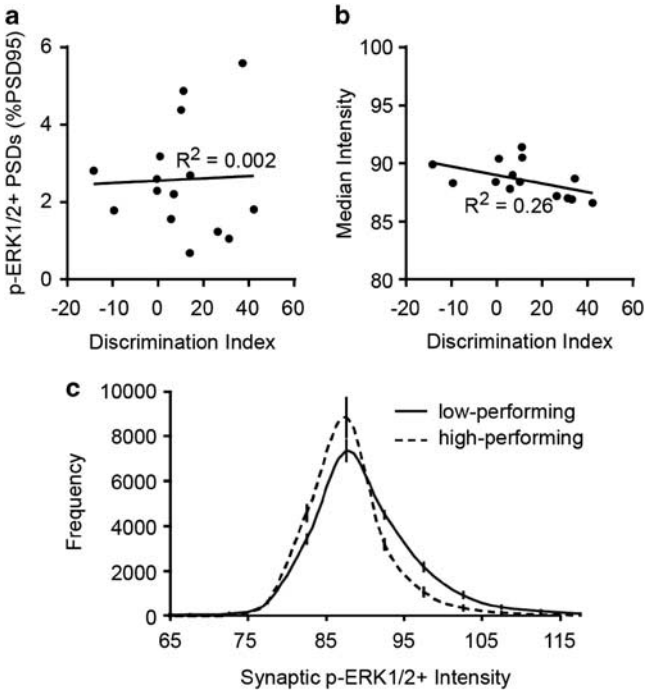

Figure 4 The synapses of BTBR mice with impaired long-term object location memory (OLM) contain more activated ERK1/2. (a) A linear regression between the number of field CA1 PSD95 + synapses containing dense p-ERK1/2 immunoreactivity and the OLM retention trial discrimination index of individual BTBR mice ($N = 15$) was not significant (Pearson correlation, $P = 0.89$; values represented as percent of total PSD95 + contacts). (b) A significant negative correlation (Pearson correlation, $R^2 = 0.26$; $P = 0.05$) was observed when comparing the median p-ERK1/2 immunolabeling intensity for elements double labeled with PSD95 with the retention trial discrimination index ($N = 15$). (c) The BTBR mice were divided into high- ($N = 5$) and low-performing ($N = 10$) groups with the latter group consisting of all BTBR mice that fell below one SD of the mean of a B6 group run alongside the BTBRs. Histograms of p-ERK1/2 immunolabeling intensities for contacts double labeled with PSD95 illustrate a rightward expansion of the intensity frequency distribution in the low-performing, relative to the high-performing, group (plot shows group mean ± SEM values).

(Baudry *et al*, 2012) and other forms of cognitive impairment (Kramar *et al*, 2012; Simmons *et al*, 2009). Here we tested effects of twice daily injections with the short half-life ampakine CX929 (5mg/kg; IP) over 4 days before 5 min OLM training (Figure 5a, left). When tested for retention 24 h following training, DIs of vehicle- and CX929-injected BTBR mice did not differ (Figure 5a, right; $P = 0.33$) and, although the mean of the vehicle group was somewhat higher than that of the BTBR cohort shown in Figure 1b, this difference was not significant (MW, $P = 0.49$). Thus, ampakine treatment did not bring BTBR performance to B6 levels.

The metabotropic glutamate receptors drive ERK1/2 activity and are necessary for memory (Lu *et al*, 1997). Abnormal mGluR5 activities in other models of autism (de Vrij *et al*, 2008; Krueger and Bear, 2011; Yan *et al*, 2005) have prompted tests of the therapeutic value of mGluR5 antagonists in BTBRs. Antagonism of mGluR5 normalizes many autism-like phenotypes in these mice, including repetitive grooming and social deficits (Silverman *et al*, 2012; Silverman *et al*, 2010a). To test if therapeutic effects extend to hippocampus-dependent OLM, B6 and BTBR mice were injected with the mGluR5 antagonist MPEP, at the same dose used in those earlier works, (5 mg/kg; IP) 30 min before OLM training (Figure 5b, left). When tested 24 h later, MPEP-treated BTBR mice had greater retention than did vehicle-treated BTBRs (two-way ANOVA, $P = 0.004$; Holm-Sidak *post hoc* analysis, BTBR veh *vs* BTBR MPEP: $P = 0.01$) and performed at levels of MPEP-treated B6 mice (Holm-Sidak *post hoc*, $P = 0.77$). Although the mean DI of the vehicle-BTBR group in this cohort was slightly higher than that of the BTBR group illustrated in Figure 1b, this difference was not significant (MW, $P = 0.83$). MPEP did not influence either strain's object exploration during training (Two-way ANOVA, $P = 0.92$) or retention testing (Two-way ANOVA, $P = 0.27$).

Because synaptic p-ERK1/2 immunolabeling intensities correlated negatively with OLM performance of individual BTBR mice, we tested whether MPEP decreases levels of synaptic p-ERK1/2 in this strain. Mice were injected with MPEP (5 mg/kg; IP) and brains were collected 30 min later. Although high- and low-performing BTBR mice were not separated here, MPEP decreased the median immunolabeling intensity of p-ERK1/2 + elements colocalized with PSD95 (87.4 ± 0.5, vehicle; 86.7 ± 0.6, MPEP; $P = 0.04$) (Figure 5c). Hill slopes at the inflection point of the fitted (Goodness of Fit $R^2 > 0.999$) cumulative fluorescence intensity distribution (Supplementary **Figure S2**) were robustly different between MPEP- and vehicle-treated BTBRs ($P = 0.0002$). As anticipated from a lack of correlation between memory performance and *numbers* of p-ERK1/2 + PSDs, this immunolabeling measure was not altered by MPEP treatment in either strain (Figure 5d). As in earlier groups (see Figure 3c), there was a significant difference in p-ERK1/2 + PSD counts between vehicle-injected B6 and BTBR mice (Two-way ANOVA, $P < 0.05$), but, importantly, there was no significant interaction between strain and treatment ($P = 0.71$).

DISCUSSION

The increasing prevalence of autism spectrum disorder associated intellectual disability underscores a critical need for mechanism-based therapeutics. Combining hippocampus-dependent OLM with fluorescence deconvolution tomography, we identified variability in learning capabilities among BTBR mice, as is also present with autism, and a strong negative correlation between learning performance and synaptic levels of activated ERK1/2. Elevated synaptic p-ERK1/2 and impaired recognition memory are also observed in a second mouse model of autism, the *Fmr1* KO model of fragile X syndrome (Seese *et al*, 2012; Ventura *et al*, 2004). Together these findings implicate ERK1/2 signaling as a possible cognition-related biomarker for multiple autism-associated disorders, although further work is needed to determine whether these synaptic results extend to more clinically accessible sites.

While many models of autism have been described (Moy *et al*, 2006; Patterson, 2011; Silverman *et al*, 2010b), the BTBR mice are unusual in that the autism-like phenotype arose spontaneously as opposed to being the result of

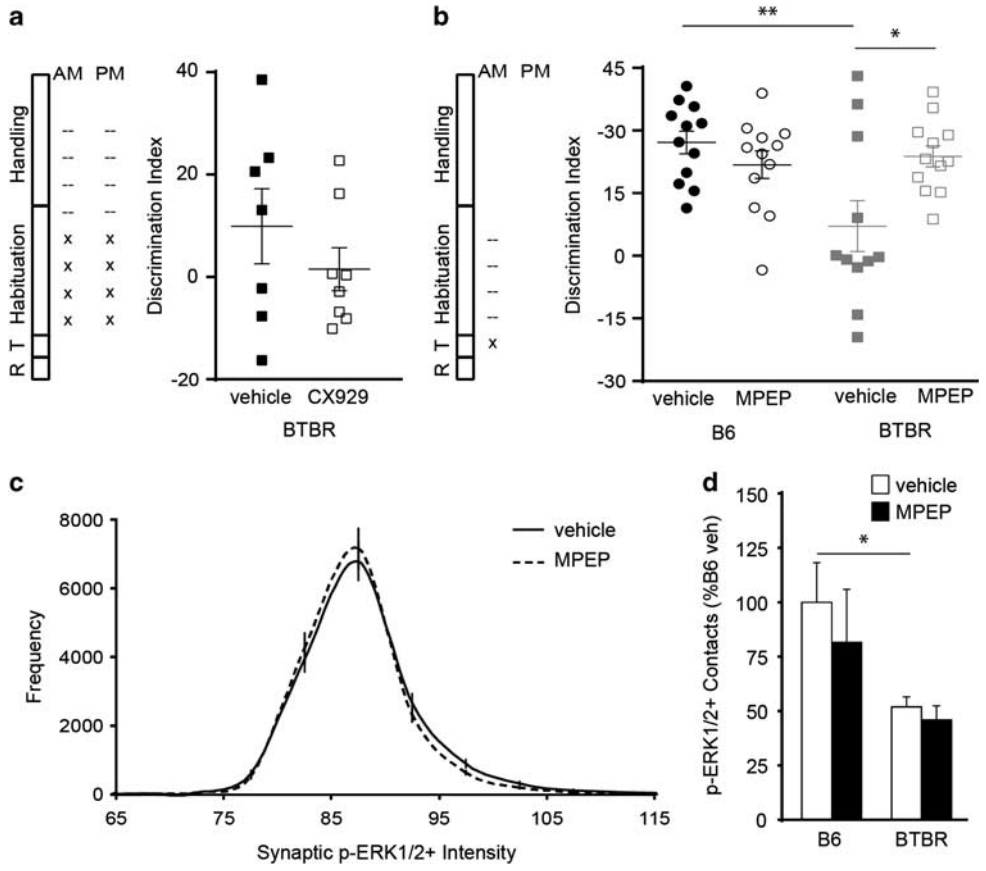

Figure 5 Metabotropic glutamate receptor 5 (mGluR5) antagonism rescues long-term memory and decreases synaptic p-ERK1/2 content in BTBR mice. (a) Left, schematic illustration of the handling and injection schedule for BTBR mice treated with 10% cyclodextrin (vehicle) or the ampakine CX929 (5 mg/kg). Starting on the morning of the second day of handling, animals received twice daily injections of vehicle for 4 days (indicated by '–'). Starting on the morning of the second day of habituation, animals received twice daily injections of either vehicle or CX929 (indicated by 'x'). The final injection occurred on the afternoon of the last day of habituation (no injections given on days of training (T) or retention (R) trials). Right, Ampakine- and vehicle-treated BTBR mice showed no significant differences in long-term memory, as measured by OLM retention trial discrimination index ($P = 0.33$; $N \geqslant 7$/group). (b) Left, treatment regimen associated with administration of the mGluR5 antagonist, MPEP, to B6 and BTBR mice. Following 4 days of once daily sterile 0.9% saline injections (indicated by '–'), which were started on the morning of the second day of habituation, MPEP (5 mg/kg) or vehicle was administered 30 min before a 5-min OLM training (T) trial (indicated by 'x'). Right, as measured by retention trial discrimination index, vehicle-treated BTBRs performed significantly worse than vehicle-treated B6s; in contrast, MPEP-treated BTBRs performed at levels of B6 mice (Holm-Sidak *post hoc* analysis, $^{*}P < 0.05$, $^{**}P < 0.01$; $N \geqslant 11$/group). (c) Immunolabeling intensity frequency distribution for p-ERK1/2+ elements double labeled for PSD95 in vehicle- and MPEP-treated BTBR mice. Note the slight leftward shift in MPEP-treated mice (group mean ± SEM values shown; $N \geqslant 11$/group). (d) Bar graph shows that the numbers of p-ERK1/2+ PSDs are lower in vehicle-treated BTBR as compared with vehicle-treated B6 mice ($^{*}P < 0.05$), and these group B6 are not affected by MPEP treatment ($N \geqslant 11$/group; values expressed as a percent of the B6 vehicle group mean).

genetic manipulation. Importantly, these mice exhibit behaviors that align with the three diagnostic criteria for autism (McFarlane *et al*, 2008; Scattoni *et al*, 2011). Although intellectual disability is not a DSMIV-specified criterion, its prevalence in autism is not trivial (Baio, 2012; Bryson *et al*, 2008; Fombonne, 2006; La Malfa *et al*, 2004). Our studies of hippocampus-dependent OLM in the BTBR strain determined that two-thirds of these mice exhibited marked impairments in OLM, whereas the remaining third performed at the levels of B6 mice. The variability in memory encoding correlated negatively with synaptic levels of activated ERK1/2, a kinase necessary for long-term memory (Thomas and Huganir, 2004). Different synaptic levels of activated ERK1/2, and potentially other kinases, might then help explain the extensive spectrum of cognitive disturbances in autism. Together, these findings strengthen the argument for using the BTBR strain as a model for features of autism that extend beyond the core autism triad to impairments in the associated symptom of cognitive impairment.

These results build on existing literature indicating that abnormal synaptic ERK1/2 signaling is associated with intellectual disability and autism. A recent study demonstrated elevated ERK1/2 phosphorylation in whole frontal cortical homogenates of BTBR mice (Zou *et al*, 2011). Many studies, including our own, have shown that synaptic ERK1/2 phosphorylation is constitutively elevated in *Fmr1* KOs (Hou *et al*, 2006; Michalon *et al*, 2012; Seese *et al*, 2012). Together with evidence for impairments in novel object recognition (Ventura *et al*, 2004), these findings suggest *Fmr1* KO mice bear similarities to the low-performing BTBRs both behaviorally and biochemically. ERK1/2 abnormalities are also observed in patients with autism: approximately 1% of cases are linked to deletions or

duplications in the gene encoding ERK1 (Kumar *et al*, 2008). A range of monogenetic autism associated disorders also involve mutations at different points in signaling through the Ras-ERK cascade (Kalkman, 2012). Furthermore, several other neurodevelopmental disorders associated with intellectual disability involve elevated ERK1/2 signaling (Samuels *et al*, 2009). More studies employing temporally constrained and both cell- and region-specific modification of ERK1/2 are warranted to understand the precise role of the kinase in cognitive deficits associated with autism.

That the BTBR mice had fewer PSDs double labeled for p-ERK1/2 is difficult to interpret in light of the increased immunolabeling intensities for contacts that were double labeled in the poor-performing BTBRs. It is possible that in the low-performing subgroup, the sparse CA1 stratum radiatum synapses containing ERK1/2 compensate by increasing its phosphorylation, a counter-productive process that is correlated with the memory encoding impairments observed here. Nonetheless, although unrelated to the poor-performing subgroup's OLM deficit, this depletion of hippocampal synapses containing measurable levels of p-ERK1/2 likely influences other BTBR phenotypes. A suggestion of relevant behaviors comes from evidence that sociability impairments, as found in BTBR mice, arise in mice with nestin-driven conditional knockout of ERK2 (McFarlane *et al*, 2008; Satoh *et al*, 2011). These results support the notion that synapses containing p-ERK1/2, either within or outside hippocampus, are critical for proper sociability, and thus the decreased density of p-ERK1/2+ synapses observed here might contribute to the BTBR's social impairments. Clearly, further characterization of this core autism-like behavior and its relationship with synaptic ERK1/2 activity is needed to understand the role of this kinase in both normal and disturbed social behavior.

Fluorescent deconvolution tomography was applied to evaluate large populations of synapses ($\sim$40 000 per sample field) and to both identify significant synaptic abnormalities associated with cognitive impairment, and provide a neurobiological measure for testing the efficacy of pharmacological treatments. MPEP is a selective, non-competitive antagonist of mGluR5, a glutamate receptor that normally increases neuronal ERK1/2 activity (Wang *et al*, 2007). Acute MPEP treatment facilitated OLM in the BTBR mice, bringing their performance to B6 levels. We propose that this effect is mediated, at least in part, by the observed MPEP-normalization of synaptic p-ERK1/2 levels. MPEP also attenuates excessive grooming in BTBR mice (Silverman *et al*, 2010a). Interestingly, ERK1/2 inhibition also decreases excessive rodent grooming (Yu and Yezierski, 2005), supporting the hypothesis that elevated synaptic p-ERK1/2 contributes to this autism-like trait in BTBR mice. Further analyses are needed to determine if synaptic p-ERK1/2 levels are abnormal and similarly responsive to MPEP treatment in grooming-related brain regions like the striatum (Langen *et al*, 2011).

Together, results presented here support the idea that in neurodevelopmental disorders the synaptic substrates of intellectual disability are meaningful targets to test the efficacy of different pharmacotherapy.

FUNDING AND DISCLOSURE

This work was supported by National Institutes of Health grants MH082042 and NS04260 and the UC Irvine Center for Autism Research and Treatment. R.R.S. was supported by grant T32-GM0862 and NIMH predoctoral fellowship FMH095432A. Drs Lynch and Gall are coauthors on patents, owned by the University of California, for the use of ampakines to support cognitive function (Lynch) and increase endogenous BDNF expression (Lynch, Gall).

ACKNOWLEDGEMENTS

We thank Chris Krook-Magnusoon and Conor Cox for valuable guidance in statistical analyses, Dr Julie C. Lauterborn for helpful discussions, and Alexander Jow, Kathleen Wang, and Yue Qin Yao for excellent technical assistance.

REFERENCES

Amodeo DA, Jones JH, Sweeney JA, Ragozzino ME (2012). Differences in BTBR T+ tf/J and C57BL/6J mice on probabilistic reversal learning and stereotyped behaviors. *Behav Brain Res* **227**: 64–72.

Aoki C, Miko I, Oviedo H, Mikeladze-Dvali T, Alexandre L, Sweeney N *et al* (2001). Electron microscopic immunocytochemical detection of PSD-95, PSD-93, SAP-102, and SAP-97 at postsynaptic, presynaptic, and nonsynaptic sites of adult and neonatal rat visual cortex. *Synapse* **40**: 239–257.

Babineau BA, Yang M, Berman RF, Crawley JN (2013). Low home cage social behaviors in BTBR T+tf/J mice during juvenile development. *Physiol Behav* **114-115C**: 49–54.

Baio J (2012). Prevalence of autism spectrum disorders-autism and developmental disabilities monitoring network, 14 sites, United States, 2008. *MMWR Surveill Summ* **61**: 1–19.

Baudry M, Kramar E, Xu X, Zadran H, Moreno S, Lynch G *et al* (2012). Ampakines promote spine actin polymerization, long-term potentiation, and learning in a mouse model of Angelman syndrome. *Neurobiol Dis* **47**: 210–215.

Belichenko PV, Kleschevnikov AM, Salehi A, Epstein CJ, Mobley WC (2007). Synaptic and cognitive abnormalities in mouse models of Down syndrome: exploring genotype-phenotype relationships. *J Comp Neurol* **504**: 329–345.

Bernard-Trifilo JA, Kramar EA, Torp R, Lin CY, Pineda EA, Lynch G *et al* (2005). Integrin signaling cascades are operational in adult hippocampal synapses and modulate NMDA receptor physiology. *J Neurochem* **93**: 834–849.

Bolivar VJ, Walters SR, Phoenix JL (2007). Assessing autism-like behavior in mice: variations in social interactions among inbred strains. *Behav Brain Res* **176**: 21–26.

Bryson SE, Bradley EA, Thompson A, Wainwright A (2008). Prevalence of autism among adolescents with intellectual disabilities. *Can J Psychiatry* **53**: 449–459.

Chen LY, Rex CS, Babayan AH, Kramar EA, Lynch G, Gall CM *et al* (2010). Physiological activation of synaptic Rac>PAK (p-21 activated kinase) signaling is defective in a mouse model of fragile X syndrome. *J Neurosci* **30**: 10977–10984.

de Vrij FM, Levenga J, van der Linde HC, Koekkoek SK, De Zeeuw CI, Nelson DL *et al* (2008). Rescue of behavioral phenotype and neuronal protrusion morphology in Fmr1 KO mice. *Neurobiol Dis* **31**: 127–132.

Fombonne E (2006). Past and Future Perspectives on Autism Epidemiology. In: Moldin S, Rubenstein J (eds). *Understanding Autism: From Basic Neuroscience to Treatment*. CRC Press Taylor & Francis: Boca Raton, FL, pp 25–48.

Haettig J, Stefanko DP, Multani ML, Figueroa DX, McQuown SC, Wood MA (2011). HDAC inhibition modulates hippocampus-dependent long-term memory for object location in a CBP-dependent manner. *Learn Mem* **18**: 71–79.

Hou L, Antion MD, Hu D, Spencer CM, Paylor R, Klann E (2006). Dynamic translational and proteasomal regulation of fragile X mental retardation protein controls mGluR-dependent long-term depression. *Neuron* **51**: 441–454.

Hung AY, Futai K, Sala C, Valtschanoff JG, Ryu J, Woodworth MA *et al* (2008). Smaller dendritic spines, weaker synaptic transmission, but enhanced spatial learning in mice lacking Shank1. *J Neurosci* **28**: 1697–1708.

Hurst JL, West RS (2010). Taming anxiety in laboratory mice. *Nat Methods* **7**: 825–826.

Kalkman HO (2012). Potential opposite roles of the extracellular signal-regulated kinase (ERK) pathway in autism spectrum and bipolar disorders. *Neurosci Biobehav Rev* **36**: 2206–2213.

Kramar EA, Chen LY, Lauterborn JC, Simmons DA, Gall CM, Lynch G (2012). BDNF upregulation rescues synaptic plasticity in middle-aged ovariectomized rats. *Neurobiol Aging* **33**: 708–719.

Krueger DD, Bear MF (2011). Toward fulfilling the promise of molecular medicine in fragile X syndrome. *Annu Rev Med* **62**: 411–429.

Kumar RA, KaraMohamed S, Sudi J, Conrad DF, Brune C, Badner JA *et al* (2008). Recurrent 16p11.2 microdeletions in autism. *Hum Mol Genet* **17**: 628–638.

La Malfa G, Lassi S, Bertelli M, Salvini R, Placidi GF (2004). Autism and intellectual disability: a study of prevalence on a sample of the Italian population. *J Intellect Disabil Res* **48**(Pt 3): 262–267.

Langen M, Kas MJ, Staal WG, van Engeland H, Durston S (2011). The neurobiology of repetitive behavior: of mice. *Neurosci Biobehav Rev* **35**: 345–355.

Lipina TV, Roder JC (2013). Co-learning facilitates memory in mice: a new avenue in social neuroscience. *Neuropharmacology* **64**: 283–293.

Lu YM, Jia Z, Janus C, Henderson JT, Gerlai R, Wojtowicz JM *et al* (1997). Mice lacking metabotropic glutamate receptor 5 show impaired learning and reduced CA1 long-term potentiation (LTP) but normal CA3 LTP. *J Neurosci* **17**: 5196–5205.

MacPherson P, McGaffigan R, Wahlsten D, Nguyen PV (2008). Impaired fear memory, altered object memory and modified hippocampal synaptic plasticity in split-brain mice. *Brain Res* **1210**: 179–188.

McFarlane HG, Kusek GK, Yang M, Phoenix JL, Bolivar VJ, Crawley JN (2008). Autism-like behavioral phenotypes in BTBR T + tf/J mice. *Genes Brain Behav* **7**: 152–163.

Meyza KZ, Defensor EB, Jensen AL, Corley MJ, Pearson BL, Pobbe RL *et al* (2013). The BTBR T + tf/J mouse model for autism spectrum disorders-in search of biomarkers. *Behav Brain Res* **251**: 25–34.

Michalon A, Sidorov M, Ballard TM, Ozmen L, Spooren W, Wettstein JG *et al* (2012). Chronic pharmacological mGlu5 inhibition corrects fragile X in adult mice. *Neuron* **74**: 49–56.

Moy SS, Nadler JJ, Magnuson TR, Crawley JN (2006). Mouse models of autism spectrum disorders: the challenge for behavioral genetics. *Am J Med Genet C Semin Med Genet* **142C**: 40–51.

Patterson PH (2011). Modeling autistic features in animals. *Pediatr Res* **69**(5 Pt 2): 34R–40R.

Ribeiro AS, Eales BA, Biddle FG (2013). Short-term and long-term memory deficits in handedness learning in mice with absent corpus callosum and reduced hippocampal commissure. *Behav Brain Res* **245**: 145–151.

Rutz HL, Rothblat LA (2012). Intact and impaired executive abilities in the BTBR mouse model of autism. *Behav Brain Res* **234**: 33–37.

Samuels IS, Saitta SC, Landreth GE (2009). MAP'ing CNS development and cognition: an ERKsome process. *Neuron* **61**: 160–167.

Satoh Y, Endo S, Nakata T, Kobayashi Y, Yamada K, Ikeda T *et al* (2011). ERK2 contributes to the control of social behaviors in mice. *J Neurosci* **31**: 11953–11967.

Scattoni ML, Ricceri L, Crawley JN (2011). Unusual repertoire of vocalizations in adult BTBR T + tf/J mice during three types of social encounters. *Genes Brain Behav* **10**: 44–56.

Seese RR, Babayan AH, Katz AM, Cox CD, Lauterborn JC, Lynch G *et al* (2012). LTP induction translocates cortactin at distant synapses in wild-type but not Fmr1 knock-out mice. *J Neurosci* **32**: 7403–7413.

Seese RR, Chen LY, Cox CD, Schulz D, Babayan AH, Bunney WE *et al* (2013). Synaptic abnormalities in the infralimbic cortex of a model of congenital depression. *J Neurosci* **33**: 13441–13448.

Silverman JL, Oliver CF, Karras MN, Gastrell PT, Crawley JN (2013). AMPAKINE enhancement of social interaction in the BTBR mouse model of autism. *Neuropharmacology* **64**: 268–282.

Silverman JL, Smith DG, Rizzo SJ, Karras MN, Turner SM, Tolu SS *et al* (2012). Negative allosteric modulation of the mGluR5 receptor reduces repetitive behaviors and rescues social deficits in mouse models of autism. *Sci Transl Med* **4**: 131ra151.

Silverman JL, Tolu SS, Barkan CL, Crawley JN (2010a). Repetitive self-grooming behavior in the BTBR mouse model of autism is blocked by the mGluR5 antagonist MPEP. *Neuropsychopharmacology* **35**: 976–989.

Silverman JL, Yang M, Lord C, Crawley JN (2010b). Behavioural phenotyping assays for mouse models of autism. *Nat Rev Neurosci* **11**: 490–502.

Simmons DA, Rex CS, Palmer L, Pandyarajan V, Fedulov V, Gall CM *et al* (2009). Up-regulating BDNF with an ampakine rescues synaptic plasticity and memory in Huntington's disease knockin mice. *Proc Natl Acad Sci USA* **106**: 4906–4911.

Thomas GM, Huganir RL (2004). MAPK cascade signalling and synaptic plasticity. *Nat Rev Neurosci* **5**: 173–183.

Tropea D, Giacometti E, Wilson NR, Beard C, McCurry C, Fu DD *et al* (2009). Partial reversal of Rett Syndrome-like symptoms in MeCP2 mutant mice. *Proc Natl Acad Sci USA* **106**: 2029–2034.

Ventura R, Pascucci T, Catania MV, Musumeci SA, Puglisi-Allegra S (2004). Object recognition impairment in Fmr1 knockout mice is reversed by amphetamine: involvement of dopamine in the medial prefrontal cortex. *Behav Pharmacol* **15**: 433–442.

Wang JQ, Fibuch EE, Mao L (2007). Regulation of mitogen-activated protein kinases by glutamate receptors. *J Neurochem* **100**: 1–11.

Wohr M, Roullet FI, Crawley JN (2011). Reduced scent marking and ultrasonic vocalizations in the BTBR T + tf/J mouse model of autism. *Genes Brain Behav* **10**: 35–43.

Yan QJ, Rammal M, Tranfaglia M, Bauchwitz RP (2005). Suppression of two major Fragile X Syndrome mouse model phenotypes by the mGluR5 antagonist MPEP. *Neuropharmacology* **49**: 1053–1066.

Yang M, Abrams DN, Zhang JY, Weber MD, Katz AM, Clarke AM *et al* (2012). Low sociability in BTBR T + tf/J mice is independent of partner strain. *Physiol Behav* **107**: 649–662.

Yang M, Zhodzishsky V, Crawley JN (2007). Social deficits in BTBR T + tf/J mice are unchanged by cross-fostering with C57BL/6J mothers. *Int J Dev Neurosci* **25**: 515–521.

Yoshii A, Constantine-Paton M (2010). Postsynaptic BDNF-TrkB signaling in synapse maturation, plasticity, and disease. *Dev Neurobiol* **70**: 304–322.

Yu CG, Yezierski RP (2005). Activation of the ERK1/2 signaling cascade by excitotoxic spinal cord injury. *Brain Res Mol Brain Res* **138**: 244–255.

Zou H, Yu Y, Sheikh AM, Malik M, Yang K, Wen G *et al* (2011). Association of upregulated Ras/Raf/ERK1/2 signaling with autism. *Genes Brain Behav* **10**: 615–624.

Supplementary Information accompanies the paper on the Neuropsychopharmacology website (http://www.nature.com/npp)